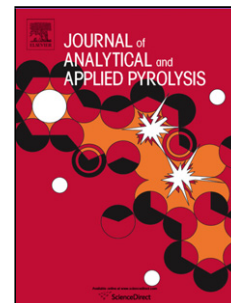


Accepted Manuscript

Title: New insights into microwave pyrolysis of biomass: preparation of carbon-based products from pecan nutshells and their application in wastewater treatment

Author: G. Duran Jimenez T. Monti J.J. Titman V.
Hernandez-Montoya S.W. Kingman E.R. Binner



PII: S0165-2370(16)30611-8
DOI: <http://dx.doi.org/doi:10.1016/j.jaap.2017.02.013>
Reference: JAAP 3972

To appear in: *J. Anal. Appl. Pyrolysis*

Received date: 30-9-2016
Revised date: 13-2-2017
Accepted date: 15-2-2017

Please cite this article as: <doi><http://dx.doi.org/10.1016/j.jaap.2017.02.013></doi>

This is a PDF file of an unedited manuscript that has been accepted for publication. As a service to our customers we are providing this early version of the manuscript. The manuscript will undergo copyediting, typesetting, and review of the resulting proof before it is published in its final form. Please note that during the production process errors may be discovered which could affect the content, and all legal disclaimers that apply to the journal pertain.

New insights into microwave pyrolysis of biomass: preparation of carbon-based products from pecan nutshells and their application in wastewater treatment

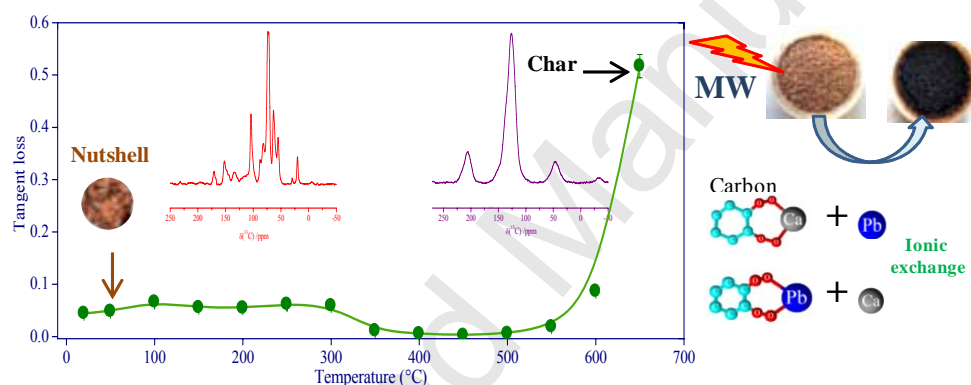
G. Duran Jimenez¹, T. Monti², J. J. Titman³, V. Hernandez-Montoya¹, S. W. Kingman², E. R. Binner²

¹Departamento de Ingeniería Química y Bioquímica, Instituto Tecnológico de Aguascalientes, 20256 Aguascalientes, México

²Microwave Process Engineering Research Group, Faculty of Engineering, University Park, University of Nottingham, Nottingham, NG7 2RD, UK

³School of Chemistry, University Park, University of Nottingham, Nottingham, NG7 2RD, UK

Graphical Abstract



Highlights

Microwave pyrolysis of nutshell to produce carbon-based products for lead removal

NMR, dielectric characterization, SEM/EDX, SBET, XRD to monitor intermediate products

Microwave leads to simultaneous (hemi)cellulosic and lignin degradation

Ion-exchange by calcium ions on the material surface promotes the lead removal

Calcium compound development directly related to microwave interaction with biomass

Abstract

Microwave pyrolysis of pecan nutshell (*Carya illinoensis*) biomass was used to produce carbon-based solid products with potential application in contaminated water treatment.

A range of analytical techniques were applied to characterize the intermediate products of microwave pyrolysis in order to monitor the physio-chemical effects of the interacting energy on the biomass.

The performance of the carbon-based products was tested through evaluation of lead ion removal capacity from solution. Further analyses demonstrated that ion-exchange by calcium ions on the material surface was the main mechanism involved in lead removal. Calcium compound development was directly correlated to the interaction of the electromagnetic waves with the biomass.

Through monitoring the physio-chemical effects of biomass-microwave interactions during microwave pyrolysis, we have shown for the first time that the intermediate products differ from those of conventional pyrolysis. We hypothesise that selective heating leads to the (hemi)cellulosic and lignin degradation processes occurring simultaneously, whereas they are largely sequential in conventional pyrolysis.

This work provides optimization parameters essential for the large scale design of microwave processes for this application as well as an understanding of how the operating parameters impact on functionality of the resulting carbon-based materials.

Keywords

Biomass; pecan nutshells; microwave pyrolysis; lead removal; ion exchange; carbon-based product

1. Introduction

Microwave treatment for biomass pyrolysis has received significant attention in the last three decades because the microwave heating mechanism has the potential to overcome several of the limitations of conventional heating. With appropriate microwave cavity configuration, energy can be transferred directly into the material, overcoming the heat transfer limitations encountered when conventionally heating low thermal conductivity materials such as biomass and leading to more even heating, shorter processing times and the ability to process larger particles [1]. Previous literature has focused upon correlating microwave parameters such as input power and irradiation time to the physio-chemical features of the final products [2]. There have been several attempts to interpret microwave processing steps in light of the dielectric properties of the biomass under treatment [3-9], the relation of the dielectric properties to the chemical and physical properties of the biomass [10] and the specific effects of the microwave interactions with matter [11-12]. In doing this, comparative analysis of the final products of microwave and conventional heating treatments were carried out [13-14]. Some studies focused on a complete understanding of the microwave process in order to control it and enable industrial scale-up. According to these studies, several hypotheses for explaining the physio-chemical transformations underpinning microwave pyrolysis were formulated and correlated to dielectric properties of the material processed. For example, in [3] and [5] the role of the absorbing phases (-OH groups in coal and water phases in ligneous biomass, respectively) were identified as responsible for the initial heating of the material. Intermediate steps, usually related to the volatilization phase [6], are difficult to interpret because of the separation of the products (gas, liquid, solid), the rapidity of the transformation and the lack of reliable and specific phase related temperature data. Furthermore, the physio-chemical transformation of the biomass during the microwave treatment leads to carbon-based solid products in which the electron mobility increases because of the formation of an increasingly ordered atomic structure [5]. This must be considered in designing appropriate microwave cavities as it has a dramatic effect on the dielectric properties of the material, which affect the electromagnetic field distribution. Selective and preferential decomposition of cellulose and hemicellulose molecules were also hypothesized to allow microwave pyrolysis at temperatures lower than in the conventional case [11-12]. Until now, these hypotheses have not been confirmed, and this paper addresses this data gap by

presenting physico-chemical analysis of the intermediate char products and relating them to the pyrolysis process.

While the gaseous and liquid products of the biomass pyrolysis are mainly employed as biofuels [4], bio char produced during microwave pyrolysis can be used in different areas such as in agriculture [15]. Due to high carbon content and its morphology, bio char can be used as asphalt binder modifier [16]. In separation processes, especially in the form of activated carbon, it can be used to remove chemicals like phenol [17] and dyes [18] and for the removal of heavy metals such as Hg, Cr, Ni [7], Cu, Cd, Zn from wastewater [19]. Furthermore, innovative applications such as super-capacitors, batteries, electrodes and hydrogen storage [20] are also possible.

Although activated carbon can be prepared from a wide range of carbon-based materials (e.g. coal and lignite), several biomass residues have been studied in order to obtain valuable products from the treatment: this is useful in recycling waste biomass that, in some cases, represent a potential environmental concern [21]. To this end, a wide range of investigations in which biomasses were used as a precursor for preparing activated carbons by employing microwave heating [22-23] can be found in the literature.

According to the Environmental Protection Agency (EPA), lead is classified as a "priority pollutant" because it is one of the most hazardous substances, with high toxicity and adverse human effects [24]. Cost-effective and selective adsorbents for toxic metals remain in high demand, especially in developing countries where ground water is commonly used for consumption [25].

The aim of the work presented in this paper was to elucidate the intermediate steps of microwave pyrolysis in order to provide optimisation data that could be used in the selection and design of microwave processes and also understand how the operating parameters impact upon the functionality of the resulting carbon-based materials. This was carried out through a case study using the conversion of a waste biomass (pecan nutshells) for the treatment of lead-contaminated water. The following objectives were set:

1. Understand and compare the physico-chemical transformations during microwave pyrolysis with conventional pyrolysis.
2. Understand the mechanism of lead adsorption onto microwave-pyrolysed material.
3. Optimise microwave pyrolysis of pecan nutshells in a 2 kW single mode microwave applicator for the production of carbon-based materials for lead removal from water, using energy requirements and adsorbent performance as optimisation parameters.

2. Experimental section

In order to meet these objectives, a single-mode microwave applicator was used to prepare activated carbon from pecan nutshell biomass. This technique is based on the high electric field intensity configuration that provides a fast transformation of the biomass sample onto carbon materials without the need for microwave susceptors [4]. The influence of microwave parameters such as input power, absorbed energy and processing time were studied.

The different physio-chemical mechanisms involved in the pyrolytic process were investigated by analysing the products of the treatments by several characterization techniques and correlating them to the measured dielectric properties. ¹³C NMR and

dielectric measurements were employed for understanding the evolution of the polysaccharides in the biomass during the treatment. Results were compared with carbon-based materials prepared via conventional heating.

A hypothetical description of the microwave treatment evolution was formulated and related to the previous literature outcomes. Understanding the evolution of the biomass under microwave processing is necessary in order to control the process, optimize it in terms of input power, treatment time, field intensity and spatial configuration.

In the second part of the paper the microwave bio char was tested for lead removal from contaminated water. The performances of the samples produced with different microwave conditions were related to absorbed energy. X-ray diffraction (XRD) was performed in order to understand the evolution of the inorganic inclusions during treatment, and textural parameters were measured, and these were correlated with lead adsorption performance. Using these methods, the adsorption mechanism mainly responsible for the lead removal by the samples was identified, and a correlation between microwave energy and lead removal was established. This further understanding is a key element for a future optimization of the microwave process for lead removal applications.

2.1 Sample preparation

Pecan nutshells (NS) were collected from an agrifood company in Mexico. The material was washed with deionized water until constant pH then dried at 70°C for 24 h, and finally milled ground and sieved to obtain a particle size of less than 1 mm.

2.2 Biomass pyrolysis systems

2.2.1 Microwave single mode high-field system

The microwave treatment system was operated at frequency of 2450 ± 25 MHz and included: a Sairem microwave generator with 2 kW maximum output power; two power sensors (Agilent U2001a) connected to the system by a bidirectional coupler (Sairem CMX50WR340) for measuring the input and reflected power; a cylindrical single mode TE010 cavity connected to the generator by a WR430 waveguide, terminated by a sliding short, and a manual 3-stub tuner to improve the impedance or power matching of the system with the generator (Fig. 1). Alumina reactors of 35 mm diameter were used to accommodate the nutshell sample within the cavity, and mullite bricks were used to support the sample. A NS sample of 30 g was weighed and placed in the reactor within the single-mode cavity. The cylindrical chimney was left open on top for accessing the sample inside the applicator and it was terminated by a sub-wavelength choking section. Nitrogen, at a flow rate of 5 L min^{-1} , was used as a sweep gas to aid the removal of volatiles and to maintain an oxygen-free atmosphere within the system. The reflected microwave power was minimized by the manual 3-stub tuner and the sliding short positioning, in order to maximize the power absorbed by the sample. A schematic diagram of the installation is shown in Fig. 1.

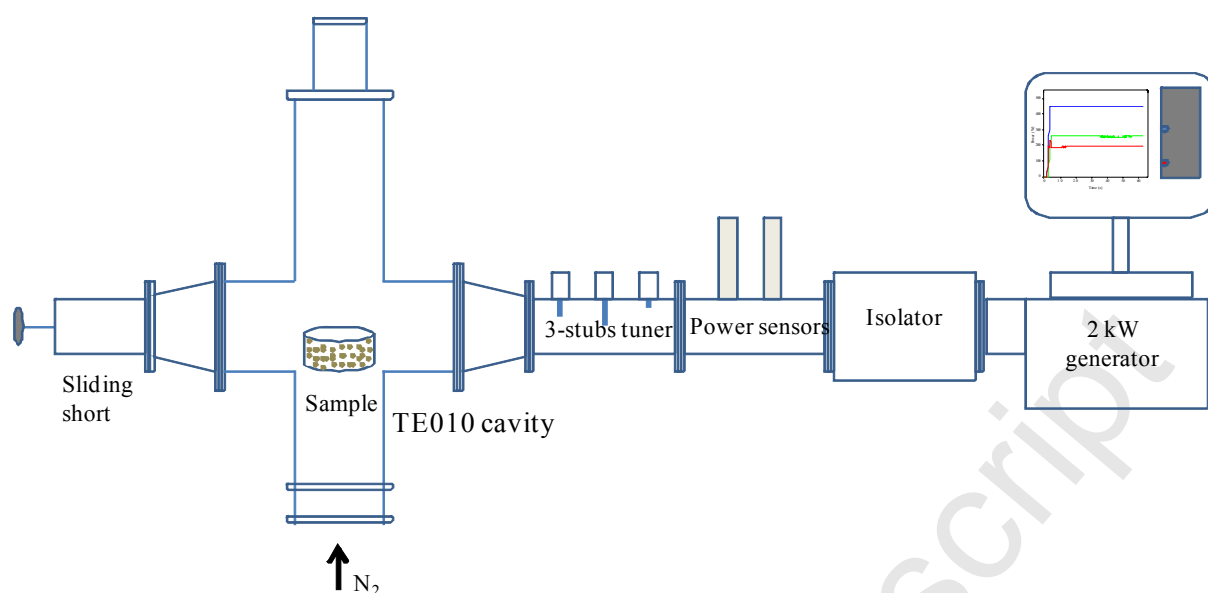


Fig. 1. Single-mode system used in the preparation of carbon-based materials: from right to left, the microwave generator, the bidirectional coupler with the power sensors, the 3-stub tuner, the single-mode cavity and the sliding short for the power matching

For the preparation of the carbon-based samples, a systematic study was carried out by varying input power and time of exposure, in order to understand the influence of these parameters on the final product quality. The total energy absorbed by the sample was determined by numerical integration of the absorbed power, which was calculated by subtracting the reflected power from the input power recorded at the input port, as described above. Twelve samples with power of 350, 450 and 550 W at irradiation times of 2, 3, 4 and 5 min were prepared. In the rest of the paper those samples are named after their preparation conditions (*e.g.* the sample prepared with 350 W input power for 2 minutes is called 'MW-350-2' and so on – see Table 1). Additionally, the surface temperature of the sample was measured by an infrared temperature gun from the open top of the cavity, immediately after each treatment; the resulting temperature values are also reported in Table 1.

Table 1. Design of experiments used in the preparation of carbon-based materials

Sample	Preparation conditions		Energy (kJ g ⁻¹)	Elemental composition				Char yield, %	Ash, %	Temp IR sensor, °C
	Input power (W)	Holding time (min)		N, %	C, %	H, %	*O, %			
MW-350-2	350	2	3.36	0.20	69.99	3.77	26.02	25.8	3.35	328
MW-350-3	350	3	4.09	0.14	82.70	0.98	16.18	23.4	7.43	335
MW-350-4	350	4	6.65	0.15	83.82	0.76	15.28	18.9	7.68	342
MW-350-5	350	5	8.33	0.17	83.79	0.52	18.03	19.5	8.36	352
MW-450-2	450	2	3.80	0.18	81.19	1.64	16.99	22.9	6.30	325
MW-450-3	450	3	5.99	0.04	83.66	0.90	15.40	20.7	7.33	329

MW-450-4	450	4	8.05	0.07	83.58	0.74	15.60	19.0	6.93	346
MW-450-5	450	5	9.97	0.13	84.83	0.56	14.48	18.6	7.36	358
MW-550-2	550	2	4.61	0.16	82.53	1.91	15.40	22.8	7.07	330
MW-550-3	550	3	7.01	0.12	83.39	0.94	14.84	21.0	7.73	349
MW-550-4	550	4	9.27	0.07	84.93	0.61	16.02	19.2	7.89	357
MW-550-5	550	5	11.71	0.15	86.07	0.49	14.12	17.8	9.02	371
NS ^a	-	-	-	0.12	50.30	5.00	43.19		1.27	-

^a The moisture content of NS is 4.9 %, obtained from the TG/DTG analysis reported in Fig. S1a (supplementary information)

^{*} Calculated by difference

It should be noted that the temperature values are just an indication of the temperature reached by the sample surface during the experiments. Microwave heating is volumetric in that the electric field penetrates the samples up to a certain depth from the surface, according to the penetration depth [26]. This quantity is a function of the microwave frequency and of the dielectric and magnetic properties. In particular, the penetration depth varies significantly during the treatment since the loss factor increases [7]. When the sample becomes more conductive the electric field penetration reduces and so the intensity inside the sample reduces and the heating becomes less homogeneous. In addition, there is more heat loss from the outside of the sample (where the measurement is taken) than the inside. For these reasons, the surface temperature values reported in this work are not representative of the temperature across the whole of the sample. Additionally, the measurement could not be taken during the experiment, so the reported values are always underestimated with respect to the temperature actually reached.

2.2.2 Conventional heating system

For comparative studies, carbon samples were also prepared using conventional heating. The thermal treatment in this latter case was carried out in a quartz reactor placed in a tubular furnace (Carbolite model CTF 12165/550). A fixed mass of 30 g of NS was heated in a nitrogen atmosphere. The temperature program comprised a heating ramp from room temperature until 350°C in one case and 650°C in the other case, at 3°C min⁻¹ and 1 h of dwell time. In this paper, we will refer to the resulting samples as CF-350 and CF-650 respectively.

2.2 Analytical techniques for samples characterization

2.2.1 Cavity perturbation technique for dielectric properties characterization

The temperature dependence of the dielectric properties of the biomass and the microwave carbonization solid-products was measured using the cavity perturbation technique at multiple frequencies. In this paper we present the results at 2470 MHz, as that is the closest to the working frequency of the microwave generator used for the following treatment. The cavity perturbation method is based on the measurement of the frequency shift from the natural resonance of the cavity and the change in quality factor after the insertion of the sample under test [27]. The measurement system used in this paper is described extensively elsewhere [5].

2.2.2 Nuclear Magnetic Resonance

¹³C CPMAS NMR spectra were recorded at room temperature on a Bruker Avance III spectrometer at a Larmor frequency of 600 MHz for ¹H using a 4 mm HXY probe spinning at 12 kHz. The spectral width was 59.5 kHz and the acquisition time was 34.4 ms. The relaxation delay was 3 s and the ¹H $\pi/2$ pulse duration was 2.9 μ s. Cross polarization

used a linear ramp from 90% to 100% of the nominal amplitude and a contact time of 2 ms. Heteronuclear decoupling was achieved by the SPINAL-64 sequence. Chemical shifts are quoted relative to TMS using adamantane as an external secondary reference.

2.2.3 Elemental and textural analysis

Characterization of the samples was performed using a range of analytical and physiochemical methods. The content of carbon, hydrogen, nitrogen and sulfur were obtained with a LECO CHNS-932 elemental analyzer. The percentage of inorganic matter (*i.e.* ash content) of the carbon samples was obtained by thermal gravimetric analysis (TGA). The samples were heated at 900°C under air atmosphere (25 ml/min) for 1 h in a TGA 5000 in TA instrument. Nitrogen adsorption isotherms were determined at 77 K using a Micromeritics ASAP 2020 sorptometer and textural properties were calculated using the appropriated models. The surface area was calculated using the Brunauer–Emmett–Teller (BET) theory, based on adsorption data in the relative pressure (P/P_0) range 0.05 to 0.3. The total pore volume was determined from the amount of nitrogen adsorbed at a relative pressure of 0.99. The micropore volume was obtained by applying the Dubinin–Raduskevich method. Additionally, Scanning Electron Microscopy (SEM) images were obtained with a FEI Quanta 600i SEM. Finally, X-ray diffraction (XRD) was collected separately with a Siemens Bruker D5000 detector, which was run in 2 theta range 10° to 80° with step size of 0.05° and step time of 10 s.

2.2.4 Lead adsorption assessment methodology

The removal efficiency of the carbons was determined by lead adsorption studies. Adsorption of Pb^{2+} from aqueous solution was studied at 30°C and pH 3 using batch systems (polycarbonate cylindrical cells with lid) with constant stirring (160 rpm). A stock solution with an initial metal concentration of 500 mg L⁻¹ was prepared by dissolving $Pb(NO_3)_2 \cdot 6H_2O$ (analytical grade) with deionized water. A defined mass of adsorbent (0.02 g) was mixed with 10 mL of aqueous metal solution for an equilibrium time of 72 h. Until equilibrium was reached, the saturated adsorbents were separated from the metal solution by decantation and the equilibrium solution was analysed by atomic absorption (AA) spectroscopy using a Perkin Elmer Analyst 100 spectrometer. Finally, the adsorbent capacity at equilibrium, q (mg/g), was calculated using a mass balance relationship given by Eq. 1:

$$q = \left(\frac{C_0 - C_e}{w} \right) V \quad (\text{Eq. 1})$$

Where C_0 and C_e are the initial and equilibrium metal concentration (mg L⁻¹), respectively, V is the volume of the metal solution (L), and W is the carbon amount (g). Additionally, the calcium concentration on equilibrium solutions (after the lead removal experiments) was determined using the same spectroscopy technique.

3. Results and discussion

3.1 Analysis for understanding microwave pyrolysis of nutshell

The dielectric properties of the biomass and their dependence with temperature were characterized and results are reported in Table 2. Several chemical reactions occurring during the sample carbonization cause significant variations of both the dielectric constant ϵ' and losses ϵ'' with temperature. Three main regions of thermal decomposition can be recognized: sample drying (up to 100-150°C), volatilization (150-400°C) and char

formation (400-600°C). The dielectric properties suddenly increase after 550°C; the remaining lignin of the nutshell is converted to char.

Table 2. Dielectric properties of nutshell biomass at 2450 Hz

Temperature, °C	Dielectric constant ϵ'	Dielectric loss factor ϵ''	Tangent loss, $\tan\delta$
20	2.402	0.107	0.045
50	2.452	0.119	0.049
100	2.615	0.173	0.066
150	2.485	0.138	0.056
200	2.494	0.137	0.055
250	2.514	0.156	0.062
300	2.360	0.140	0.059
350	1.795	0.020	0.011
400	1.720	0.010	0.006
450	1.668	0.005	0.003
500	1.638	0.010	0.006
550	1.646	0.031	0.019
600	1.733	0.150	0.087
650	2.389	1.236	0.517

These results are in accordance with those previously reported in literature for different kinds of ligneous biomasses [3-4] and coal [5, 8]. The temperatures at which the different phases commence can vary between the chosen biomasses and is strongly depend on their typical chemical functionalities [28]. In this sense, NS have been reported to comprise cellulose (29.54%), hemicellulose (25.87%), lignin (40.50%) and soluble compounds (4.09%) [29-30] with a proximate analysis of volatile matter (84.41%), fixed carbon (10.8%), moisture (3.6%) and ash (1.27%) [31]. The reported value for NS moisture content is also similar to the data obtained in this work by TG/DTG analysis (4.9%) (see supplementary information, Fig. S1a).

In order to compare the decomposition process occurring during the microwave treatment and conventional, the sample prepared under microwaves at lower power and for a lower exposure time, MW-350-2, and the conventional samples, CF-350 and CF-650, were tested and their features compared to the raw material, NS. Fig. 2 shows the ^{13}C NMR analysis obtained in order to investigate chemical changes that the material experiences during thermal decomposition. Other microwave samples were tested but their spectra are not reported since they exhibited the same features as CF-650. In general, there is significant overlap between the hemicellulose and the cellulose peaks, as well as with the lignin side chain, but we can say that some of the carbon-13 peaks are signatures of a particular species. In this way,

- 1) Cellulose can be identified by the anomeric carbon signal at 105.5 ppm.
- 2) Hemicellulose by the acetate signals at 171.6 and 21.0 ppm. For hemicellulose the anomeric carbon is a shoulder at 102 ppm.
- 3) Lignin can be identified by the methoxy signal at 56.1 ppm and the aromatic resonances between 110 and 160 ppm.

These assignments are in good agreement with the literature [32]. The untreated nutshell spectrum of Fig. 2 contains all of these signature peaks. After conventional heating at 350°C, all of the cellulose and hemicellulose peaks vanished the anomeric

carbons at 105.5 and 102 ppm and the rest of the saccharide peaks between 64.2 and 88.6 ppm, as well as the hemicellulose acetate peaks at 171.6 and 21.0 ppm, showing that both the hemicellulose and the cellulose were decomposed. The lignin aromatics at 135 to 160 ppm and the methoxy at 56.1 ppm are still present. However, the peaks from the lignin 3-carbon linkage which should appear between 70 and 80 ppm have also vanished. The lack of lignin intensity between 70 and 80 ppm suggests that the lignin broke down into its (more stable) aromatic parts - as expected, since the combustion products of lignin are methoxy phenol compounds. The remainder of the spectrum of CF-350 is a new contribution centred around 128 ppm (with sidebands at 208 ppm and 49 ppm), which is the (poly)aromatic end-product of the char process. The latter contribution is all that remains in the spectrum of CF-650. However, the spectrum of MW-350-2 (lowest power, shortest time) shows all of the distinctive peaks (1-3) listed above. There are some changes to the aromatic region with the dominant feature at 146 ppm reminiscent of the CF-350 spectrum. This suggests the lignin decomposed to methoxy phenol again, but the hemicellulose and the cellulose remained.

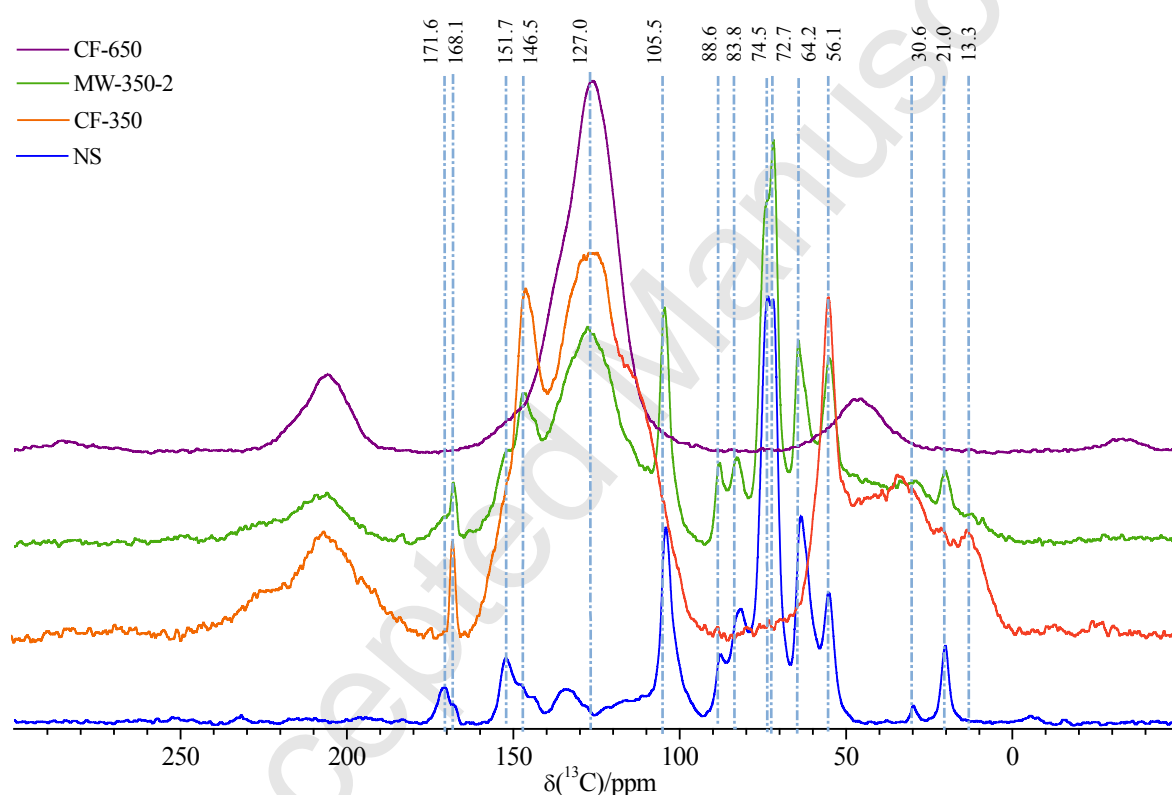


Fig. 2. ^{13}C NMR analysis of NS (blue), CF-350 (red), MW-350-2 (green) and CF-650 (purple)

Results are confirmed by TG/DTG analyses where a residual amount of (hemi)cellulose is still present in MW-350-2, but it is absent in CF-350 (Suppl. info – Fig. S1).

The disparity in composition between CF-350 and MW-350-2 indicates that although the surface temperature of MW-350-2 (of 328°C) approached the bulk temperature of CF-350 (350°C), there were temperature gradients present in the microwaved sample, and some parts of the sample did not reach (hemi)cellulose decomposition temperatures. The ^{13}C NMR analysis reported here cannot determine whether the sample is heterogeneous on a macroscopic scale or a more homogeneous mixture on a molecular level. Therefore, this heterogeneity in sample composition could be caused by uneven heating caused by electric field variation across the cavity in relation to the limited size of the samples, the particle size range and the natural porosity of the sample itself; additionally selective heating of specific phases within the sample can occur. If the latter

is true, several possible hypotheses can be proposed to explain the heterogeneity in sample composition: at the start of the microwave treatment, the water phases (the only microwave absorbers at room temperature) superheat because of the high electric field applied, reaching sufficient temperatures to decompose cellulose, hemicellulose and lignin locally due to poor heat transfer properties of the particles, leaving some residual cellulose and hemicellulose. Even though we cannot directly measure the bulk temperature of the sample, we observe that other conversions that would occur at higher temperatures did not happen. Alternatively, selective microwave interactions with (hemi)cellulose molecules [11-12] or with potentially derived products (e.g. anhydrocellulose and levoglucosan) [33] could occur in the region between 350 and 600°C. As reported in previous literature [3], the localized formation of char generates a positive feedback in the microwave absorbance process, by increasing the material losses and promoting a further increase of temperature. In this way, adjacent areas could reach high temperature as well, by different heating mechanisms, and thus producing uniformly treated samples.

In order to exclude selective heating of the remaining inorganic components [19, 31], dielectric measurements of these compounds were performed to determine if they were readily heated within a microwave field. They were mainly identified as calcium oxalate (CaC_2O_4) and the derivative of its thermal degradation (CaCO_3 and CaO). Results provide no evidence of selective heating of such compounds with respect to the rest of the sample components (Suppl. Info – Fig. S2). The loss tangent, $\tan\delta = \epsilon''/\epsilon'$, of the calcium-based components in fact is <0.1 for the entire range of temperature under test [34]. It is likely that the chemical evolution of these compounds is induced by the increasing temperature in the surrounding organic components, showing overall higher $\tan\delta$ than the calcium-based compounds.

In order to characterize the different products of the microwave and conventional pyrolysis of NS biomass, dielectric measurements were performed on the two conventional samples (CF-350, CF-650) and on several of the microwave samples (MW-350-2, MW-350-3 and MW-450-2).

It is possible to compare the dielectric results of Fig. 3 with the observations based on ^{13}C NMR results: the MW-350-2 sample (lower microwave energy) is dielectrically similar to CF-350, while it is very different from both MW-350-3 and MW-450-2, similarly to the NMR case. The dielectric features of CF-650 are more similar to MW-350-2 and CF-350 rather than MW-350-3 and MW-450-2, conversely to their ^{13}C NMR spectra. These results are in good agreement with the outcomes of a previous work from [13] where microwave pyrolysis was found to produce more char than the conventional one. Char in fact has a relatively high conductivity that increases when heated at higher temperature. This is likely due to the re-ordering of the carbon structure to more plate-like graphitized aromatic sheets [5]. Even though the (poly)aromatic end products in the CF-650, MW-350-3, MW-450-2 look similar in the NMR spectra, their structure is likely to be different. Higher microwave energy input results in a more ordered (and so more conductive) structure, which is consistent with our inability to tune the NMR probe for ^1H with samples subjected to higher microwave powers. It is noted that after 300°C, further char starts forming in the sample during analysis from a remaining part still not carbonized. In Fig. 3, the higher losses of MW-450-2 after 300°C are due to this further transformation; MW-450-2 (3.8kJ g^{-1}) had more unreacted components than MW-350-3 (4.09kJ g^{-1}).

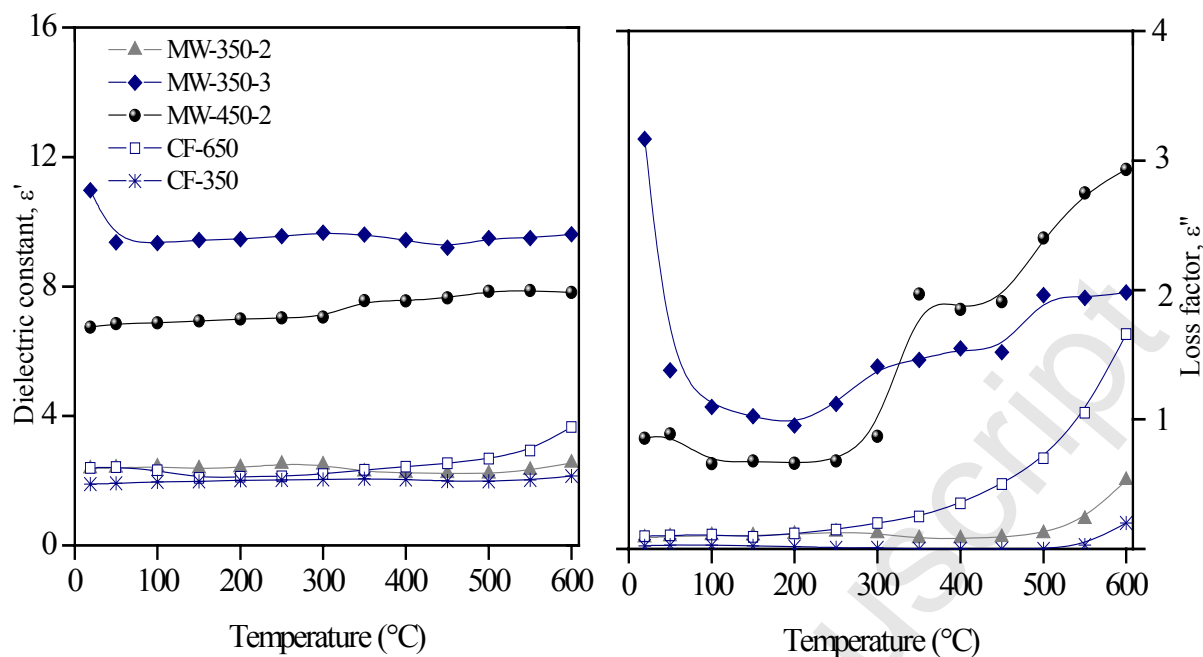


Fig. 3. Comparison between dielectric properties of carbon samples produced by microwave treatment at different conditions (MW-350-2, MW-350-3, MW-450-2), by conventional heating at 650°C (CF-650) and 350°C (CF-350)

3.2 Application of the carbon based products in lead removal from aqueous solution

The carbon-based samples obtained from the microwave treatment were tested against the lead removal capacity from aqueous solution. As described in the introductory section, this is one of the possible applications of the bio-char. It is well known that the heavy metal removal in water depends on: 1) physio-chemical features of the adsorbents; 2) chemical properties of the ions in solution. The specific surface area and porous structure have been described as the most important characteristics in carbon adsorbents that determine its successful application in pollutant removal from water [23].

In order to investigate the role of the porous structure and surface area on Pb^{2+} removal, specific surface area (S_{BET}) and nitrogen isotherms were determined. Furthermore, Fig. 4a illustrates the lead removal onto carbon-based materials produced by microwave treatment. The lead removal shows a clear correlation with microwave energy input in Fig. 4, and this does not correlate with the specific surface area (see Fig. 5). Although specific surface area increases on initial exposure to microwaves, further microwave treatment results in a loss of specific surface area; this energy threshold appears to be around 6 kJ/g for all three microwave input powers. Higher power treatments at the same total energy input also seem to yield lower specific surface area results. One possible explanation for this behaviour could be related to the fact that with high absorbed energy and powers, overheating degrades and melts the microporous structure, leaving mesoporous material. Specific data of micro- and mesoporosity percentages are reported in the supplementary information (Table S1).

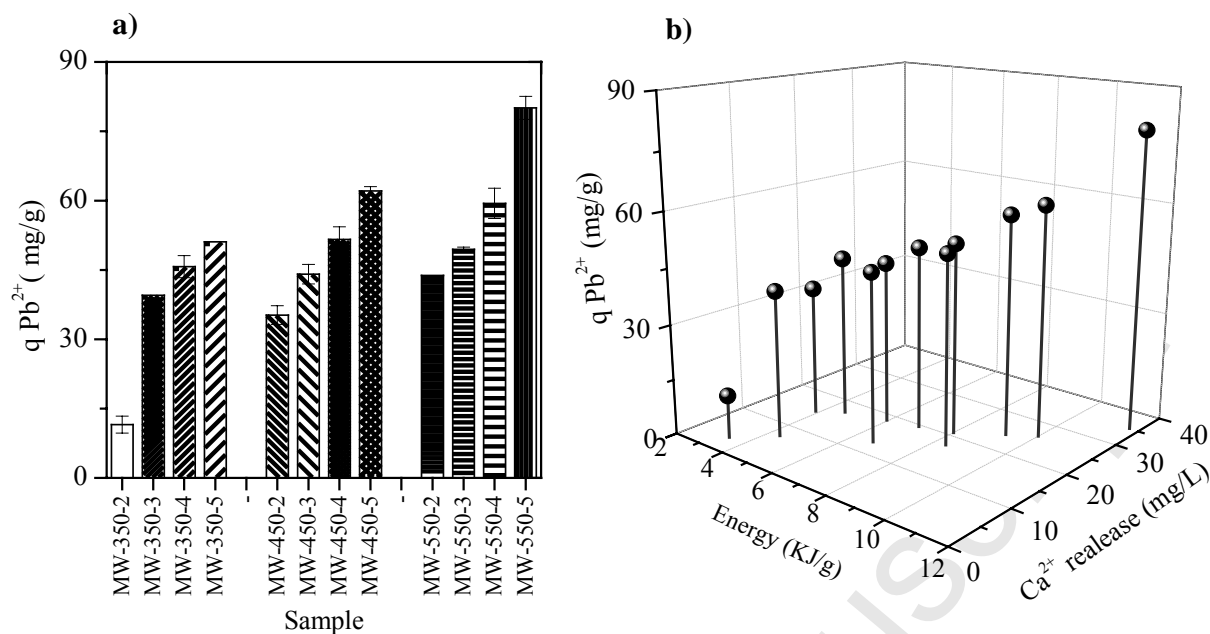


Fig. 4. Lead removal onto carbon-based samples prepared under microwave heating (a) and plot of the relationship between the absorbed microwave energy and calcium released in solution (b)

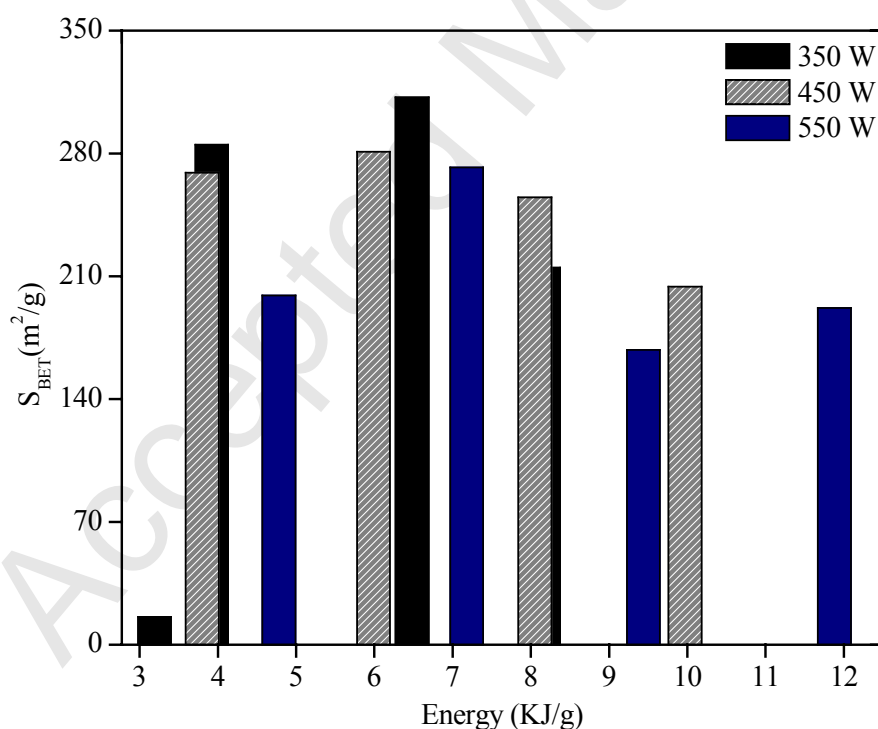


Fig. 5. Specific surface area (S_{BET}) as function of the energy absorbed during the treatment

It is therefore apparent that the surface area and porosity of the materials were not the predominant factor determining lead removal efficiency. By comparing the ash contents in Table 1 and the lead removal performance, a relationship was found in that the samples with higher ash content demonstrated better lead removal. The most prevalent element in the inorganic portion of the carbon samples is the calcium, and the basicity of carbon samples can be conditioned by this element [19]. In order to evaluate the

possible relationship of inorganic matter with adsorption removal, the calcium concentration in equilibrium solutions (after the lead removal experiments) was determined. Interestingly, the results illustrate that the samples showing higher levels of lead removal are the samples with the higher calcium liberation in solution. Fig. 4b clearly highlights such a correlation.

In order to further investigate the lead removal mechanism, XRD and Scanning Electron Microscopy/Energy Dispersive using X-Ray analysis (SEM/EDX) were carried out on samples MW-450-5 and MW-550-5 before and after the lead removal experiment, and the loaded samples were called MW-450-5-L and MW-550-5-L respectively. Results for MW-450-5 and MW-450-5-L were similar to those for MW-550-5 and MW-550-5-L, and therefore are presented in supplementary Fig. S3 and Fig S4 and will not be discussed separately. The results for MW 550-5 before and after lead removal are reported in Fig. 6.

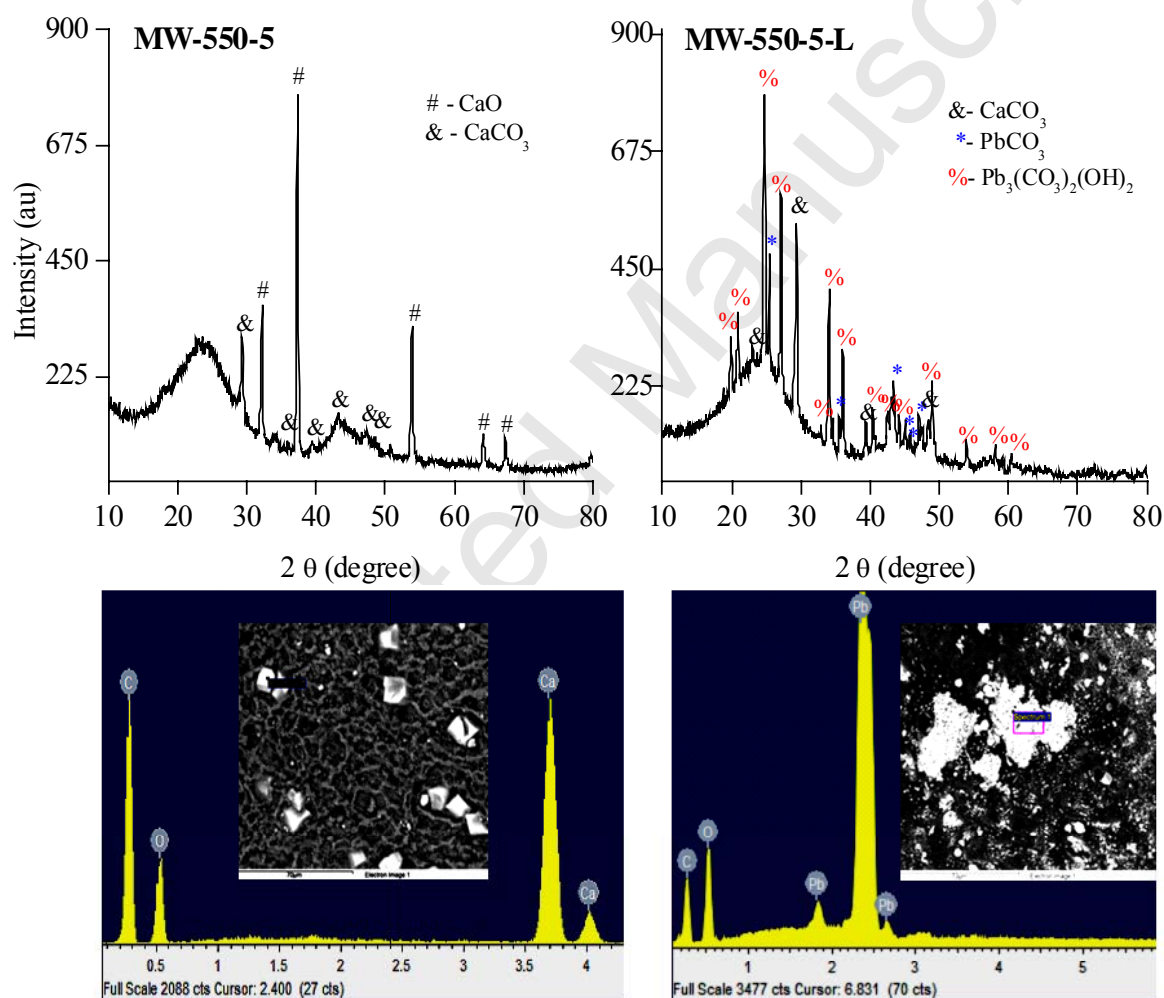
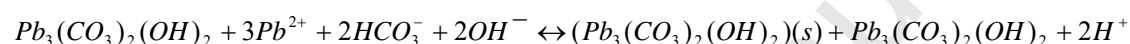
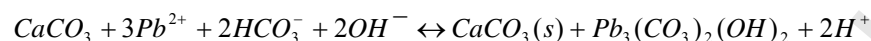
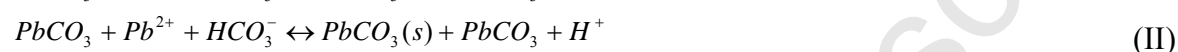
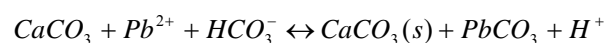


Fig. 6. SEM/EDX and XRD of the carbon-based samples MW-550-5 and of the same sample loaded with Pb²⁺ (MW-550-5-L)

Fig. 6 confirms that the precipitate onto the sample surface is composed of lead crystals (in two forms, prismatic and tabular hexagonal). Punctual composition, tested by EDX and XRD diffractogram, consists of cerussite (PbCO₃) and hydrocerussite [Pb₃(CO₃)₂(OH)₂]. Additionally, the EDX spectrum of the sample before lead removal (MW-550-5), shows characteristic peaks of C, O and Ca elements only, while in the loaded sample (MW-550-5-L) spectrum a distinctive peak for lead appears. This further

corroborates the hypothesis of the formation of this compound as the association of calcium carbonate and oxide with lead ions directly on the surface of the carbon sample. It should be noticed that there is a direct relationship between the amount of Ca detected by XRD and the adsorption capacities of the carbon-based materials analysed. Additionally, the surface lead precipitation can be corroborated as the pH equilibrium solution which increased at values of ~6 where the lead precipitation occurs. On the other hand, the generic term 'sorption' is referred to transfer ions from aqueous solution to solid surface, which includes surface adsorption or complexation, surface precipitation and ion exchange [35]. On the basis described before, the lead removal can occur through mechanisms as: ion-exchange by calcium ion in the surface of material, which refers to outer-sphere complexation (I) and precipitation of metallic ion onto carbon material (II) [36].



The conversion of the starting calcium oxalate in calcium carbonate and finally in calcium oxide was also observed by comparing the XRD spectra of the NS and the microwave samples. Distinctive peaks for the CaC_2O_4 progressively disappeared with higher microwave absorbed energy while new peaks of the $CaCO_3$ and CaO were formed (Suppl. info – Fig. S5).

Interestingly, the XRD spectra also showed an increasing order in the carbon structure with higher absorbed energy. The broad peak between 10° and 30° in the NS spectra becomes narrow in the microwave samples and it is narrower with higher treating energy. In fact, in MW-550-5 this peak is well confined between 20° and 30° .

This further confirms the hypothesis around the sample evolution under microwave treatment detailed in the previous paragraph and supported by NMR and dielectric analyses.

4. Conclusions

A single-mode microwave applicator has been used to prepare activated carbon from pecan nutshell biomass without the addition of microwave susceptors. The influence of microwave processing parameters (input power, absorbed energy and processing time) on the physico-chemical characteristics and lead removal performance of the carbon-based products was determined, and these results were compared with carbon-based materials prepared via conventional heating.

The results show that intermediate products during microwave pyrolysis differ from those of conventional pyrolysis. Selective heating leads to (hemi)cellulosic and lignin degradations occurring simultaneously, whereas they are largely sequential in conventional pyrolysis. Microwave heating at higher energy inputs ($> 4\text{ kJ/g}$) results in a more ordered char structure than conventional heating up to 650°C , and this appears to correspond with an increase in dielectric loss above 550°C enabling a rapid increase in heating rate.

The specific surface area of the carbon-based materials increases on initial exposure to microwaves, but further microwave treatment results in a loss of specific surface area at an energy threshold of around 6 kJ/g . Higher power treatments at the same total energy input also seem to yield lower specific surface area results. This behaviour could be related to the fact that with high absorbed energy and powers, overheating degrades

and melts the microporous structure, leaving mesoporous material. However, the results show that the surface area and porosity of the materials are not the predominant factor determining lead removal efficiency. The calcium components present on chars prepared by microwave heating play a crucial role in the effective removal of lead, and in fact ion-exchange by calcium ions on the material surface is the main mechanism involved in lead removal. Calcium compound development and lead removal performance directly correlate with the microwave energy input.

Finally, this work provides data useful for estimating the parameters for the large scale design of microwave processes and an understanding of how the operating parameters impact on functionality of the resulting carbon-based materials. The highest lead removal of 80.3 mg/g was achieved at the highest energy input of 11.7 kJ/g. However, further optimization of the treatment parameters to prevent loss of surface area while still maximising calcium compound development could lead to further improvements in the materials' performance.

References

- [1] Krieger-Brockett, B. (1994). Microwave pyrolysis of biomass. *Res Chem Intermedia*, 20(1), 39-49.
- [2] Guo, J., Lua, A. C. (2000). Preparation of activated carbons from oil-palm-stone chars by microwave-induced carbon dioxide activation. *Carbon*, 38, 1985-1993.
- [3] Robinson, J. P., Kingman, S. W., Barranco, R., Snape, C. E., Al-Sayegh, H. (2010). Microwave pyrolysis of wood pellets. *Ind Eng Chem Res*, 49(2), 459-463.
- [4] Robinson, J., Dodds, C., Stavrinides, A., Kingman, S., Katrib, J., Wu, Z., Overend, R. (2015). Microwave pyrolysis of biomass: control of process parameters for high pyrolysis oil yields and enhanced oil quality. *Energy Fuel*, 29(3), 1701-1709.
- [5] Lester, E., Kingman, S., Dodds, C., Patrick, J. (2006). The potential for rapid coke making using microwave energy. *Fuel*, 85(14), 2057-2063.
- [6] Binner, E., Mediero-Munoyerro, M., Huddle, T., Kingman, S., Dodds, C., Dimitrakakis, G. E., Lester, E. (2014). Factors affecting the microwave coking of coals and the implications on microwave cavity design. *Fuel Process Technol*, 125, 8-17.
- [7] Tripathi, M., Sahu, J. N., Ganesan, P., Dey, T. K. (2015). Effect of temperature on dielectric properties and penetration depth of oil palm shell (OPS) and OPS char synthesized by microwave pyrolysis of OPS. *Fuel*, 153, 257-266.
- [8] Peng, Z., Hwang, J.-Y., Kim, B.-G., Mouris, J., Hutcheon, R. (2012). Microwave absorption capability of high volatile bituminous coal during pyrolysis. *Energy Fuel*, 26 (8) 5146- 5151.
- [9] Motasemi, F., Salema, A. A., Afzal, M. T. (2015). Dielectric characterization of corn stover for microwave processing technology. *Fuel Process Technol*, 131, 370-375.

- 611 [10] Sait, H. H., Salema, A. A. (2015). Microwave dielectric characterization of Saudi
612 Arabian date palm biomass during pyrolysis and at industrial frequencies. *Fuel*, 161,
613 239-247.
- 614 [11] Budarin, V. L., Clark, J. H., Lanigan, B. A., Shuttleworth, P., Macquarrie, D. J.
615 (2010). Microwave assisted decomposition of cellulose: A new thermochemical route for
616 biomass exploitation, *Bioresource Technol*, 101(10), 3776-3779.
- 617 [12] Budarin, V. L., Shuttleworth, P. S., De Bruyn, M., Farmer, T. J., Gronnow, M. J.,
618 Pfaltzgraff, L., Macquarrie, D. J., Clark, J. H. (2015). The potential of microwave
619 technology for the recovery, synthesis and manufacturing of chemicals from bio-wastes,
620 *Catal Today*, 239(1), 80-89.
- 621 [13] Wu, C., Budarin, V. L., Gronnow, M. J., De Bruyn, M., Onwudili, J. A., Clark, J. H.,
622 Williams, P. T. (2014). Conventional and microwave-assisted pyrolysis of biomass under
623 different heating rates. *J Anal Appl Pyrol*, 107, 276-283.
- 624 [14] Alslaibi, T. M., Abustan, I., Ahmad, M. A., Foul, A. A. (2014). Microwave
625 irradiated and thermally heated olive stone activated carbon for nickel adsorption from
626 synthetic wastewater: a comparative study. *AIChE J*, 60(1), 237-250.
- 627 [15] Malghani, S., Gleixner, G., Trumbore, S. E. (2013). Chars produced by slow
628 pyrolysis and hydrothermal carbonization vary in carbon sequestration potential and
629 greenhouse gases emissions. *Soil Biol Biochem*, 62, 137-146.
- 630 [16] Zhao, S., Huang, B., Ye, X. P., Shu, X., Jia, X. (2014). Utilizing bio-char as a bio-
631 modifier for asphalt cement: A sustainable application of bio-fuel by-product. *Fuel*, 133,
632 52-62.
- 633 [17] Liu, W. J., Zeng, F. X., Jiang, H., Zhang, X. S. (2011). Preparation of high
634 adsorption capacity bio-chars from waste biomass. *Bioresource Technol*, 102(17), 8247-
635 8252.
- 636 [18] Ramirez-Montoya, L. A., Hernandez-Montoya, V., Montes-Moran, M. A. (2014).
637 Optimizing the preparation of carbonaceous adsorbents for the selective removal of
638 textile dyes by using Taguchi methodology. *J Anal Appl Pyrol*, 190, 9-20.
- 639 [19] Durán-Jiménez, G., Hernández-Montoya, V., Montes-Morán, M. A., Rangel-
640 Méndez, J. R., & Tovar-Gómez, R. (2016). Study of the adsorption-desorption of Cu^{2+} ,
641 Cd^{2+} and Zn^{2+} in single and binary aqueous solutions using oxygenated carbons prepared
642 by Microwave Technology. *J Mol Liq*, 220, 855-864.
- 643 [20] Sevilla, M., Mokaya, R. (2014), Energy storage applications of activated carbons:
644 supercapacitors and hydrogen storage. *Energy Environ Sci*, 7, 1250-1280.
- 645 [21] Pfaltzgraff, L. A., Cooper, E. C., Budarin, V., Clark, J. H. (2013). Food waste
646 biomass: a resource for high-value chemicals. *Green Chem*, 15(2), 307-314.

- 647 [22] Alslaibi, T. M., Abustan, I., Ahmad, M. A., Foul, A. (2013). A review: production of
648 activated carbon from agricultural byproducts via conventional and microwave heating. J
649 Chem Technol Biotechnol, 88(7), 1183–1190.
- 650 [23] Hesas, R. H., Daud, W. M. A. W., Sahu, J. N., Arami-Niy, a A. (2013). The effects
651 of a microwave heating method on the production of activated carbon from agricultural
652 waste: a review. J Anal Appl Pyrol, 100, 1-11.
- 653 [24] Ghasemi, M., Naushad, M., Ghasemi, N., Khosravi-fard, Y. (2013). A novel
654 agricultural waste based adsorbent for the removal of Pb (II) from aqueous solution:
655 Kinetics, equilibrium and thermodynamic studies. J Ind Eng Chem 20 (2), 454-461.
- 656 [25] Li, K., Wang, X. (2009). Adsorptive removal of Pb(II) by activated carbon
657 prepared from *Spartina alterniflora*: Equilibrium, kinetics and thermodynamics.
658 Bioresource Technol, 100, 2810–2815.
- 659 [26] Mehdizadeh, M. (2009). Single-mode Microwave Cavities for Material Processing
660 and Sensing. Microwave/RF Applicators and Probes for Material Heating, Sensing, and
661 Plasma Generation, ch.1. Boston, William Andrew Publishing.
- 662 [27] Slocombe, D., Porch, A., Bustarret, E., William, O.A. (2013). Microwave
663 properties of nanodiamond particles. Appl Phys Lett, 102, 244102.
- 664 [28] Miura, K., Mae, K., Sakurada, K., Hashimoto, K. (1992). Flash pyrolysis of coal
665 following thermal pretreatment at low temperature. Energy&Fuels, 6 (1), 16-21.
- 666 [29] Demirbas, A. (2004). Combustion characteristics of different biomass fuels. Prog
667 Energ Combust, 30(2), 219-230.
- 668 [30] Prado, A. C. P. do, Manion, B. A., Seetharaman, K., Deschamps, F. C., Arellano,
669 D. B., Block, J. M. (2013). Relationship between antioxidant properties and chemical
670 composition of the oil and the shell of pecan nuts [*Carya illinoensis* (Wangenh) C.
671 Koch]. Ind Crop Prod, 45, 64– 73.
- 672 [31] Aguayo-Villarreal, I.A., Ramírez-Montoya, L.A., Hernández-Montoya, V., Bonilla-
673 Petriciolet, A., Montes-Morán, M.A., Ramírez-López, E.M. (2013). Sorption mechanism of
674 anionic dyes on pecan nut shells (*Carya illinoensis*) using batch and continuous
675 systems, Ind Crop Prod 48 89–97.
- 676 [32] Preston, C. M., Sayer, B. G. (1992). What's in a nutshell: an investigation of
677 structure by carbon-13 cross-polarization magic-angle spinning nuclear magnetic
678 resonance spectroscopy. J Agric Food Chem, 40, 206–210.
- 679 [33] Mohan, D., Pittman, C. U. Jr, Steele, P. H. (2006). Pyrolysis of wood/biomass for
680 bio-oil. A critical review. Energy&Fuels, 20(3), 848-889.
- 681 [34] Saxena, V. K., Chandra, U. (2011) Microwave synthesis: a physical concept.
682 INTECH Open Access Publisher.

[35] Zhu, Ch. (2002). Estimation of surface precipitation constants for sorption of divalent metals onto hydrous ferric oxide and calcite, *Chemical Geology*, 188, 23– 32.

[36] Mlayah, A., Jellali, S. (2015). Study of continuous lead removal from aqueous solutions by marble wastes: efficiencies and mechanisms. *Int J Environ Sci Tech*, 12, 2965-2978.

Captions

Fig. 1 Single-mode system used in the preparation of carbon-based materials: from right to left, the microwave generator, the bidirectional coupler with the power sensors, the 3-stub tuner, the single-mode cavity and the sliding short for the power matching.

Fig. 2 ^{13}C NMR analysis of NS (blue), CF-350 (red), MW-350-2 (green) and CF-650 (purple)

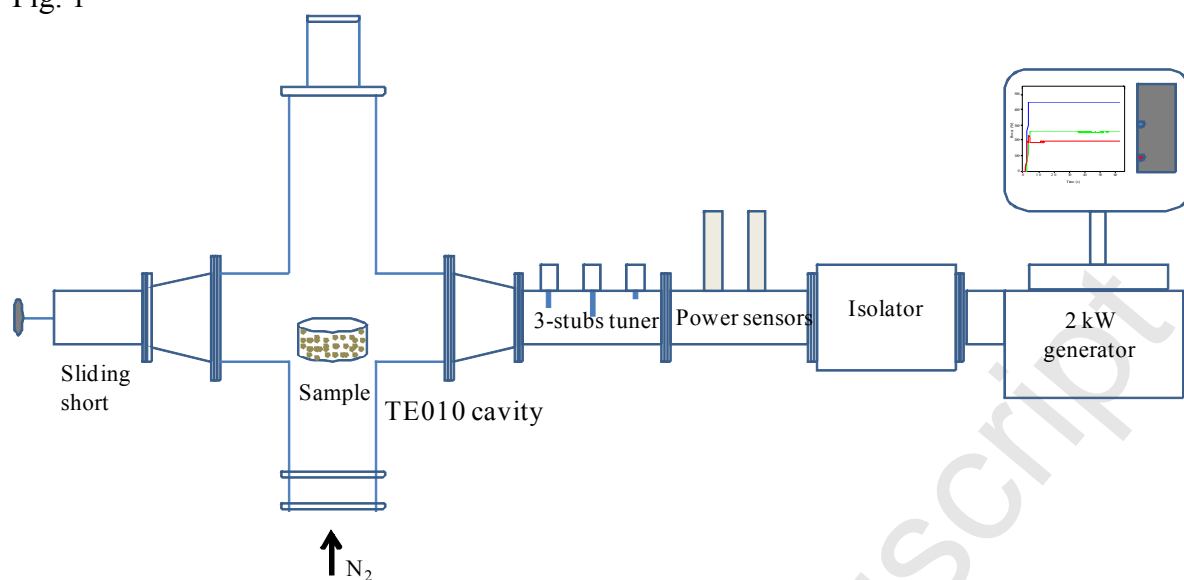
Fig. 3 Comparison between dielectric properties of carbon-based samples produced by microwave treatment at different conditions (MW-350-2, MW-350-3, MW-450-2), and by conventional heating (CF-650 and CF-350).

Fig. 4 Lead removal onto carbon-based samples prepared under microwave heating (a) and plot of the relationship between the absorbed microwave energy and calcium released in solution (b).

Fig. 5 Specific surface area (S_{BET}) as function of the energy absorbed during the treatment.

Fig. 6 SEM/EDX and XRD of the carbon-based samples MW-550-5 and of the same sample loaded with Pb^{2+} (MW-550-5-L).

711 Fig. 1



712
713
714
715
716
717
718
719
720
721
722
723
724
725
726
727
728
729
730
731

Fig. 2

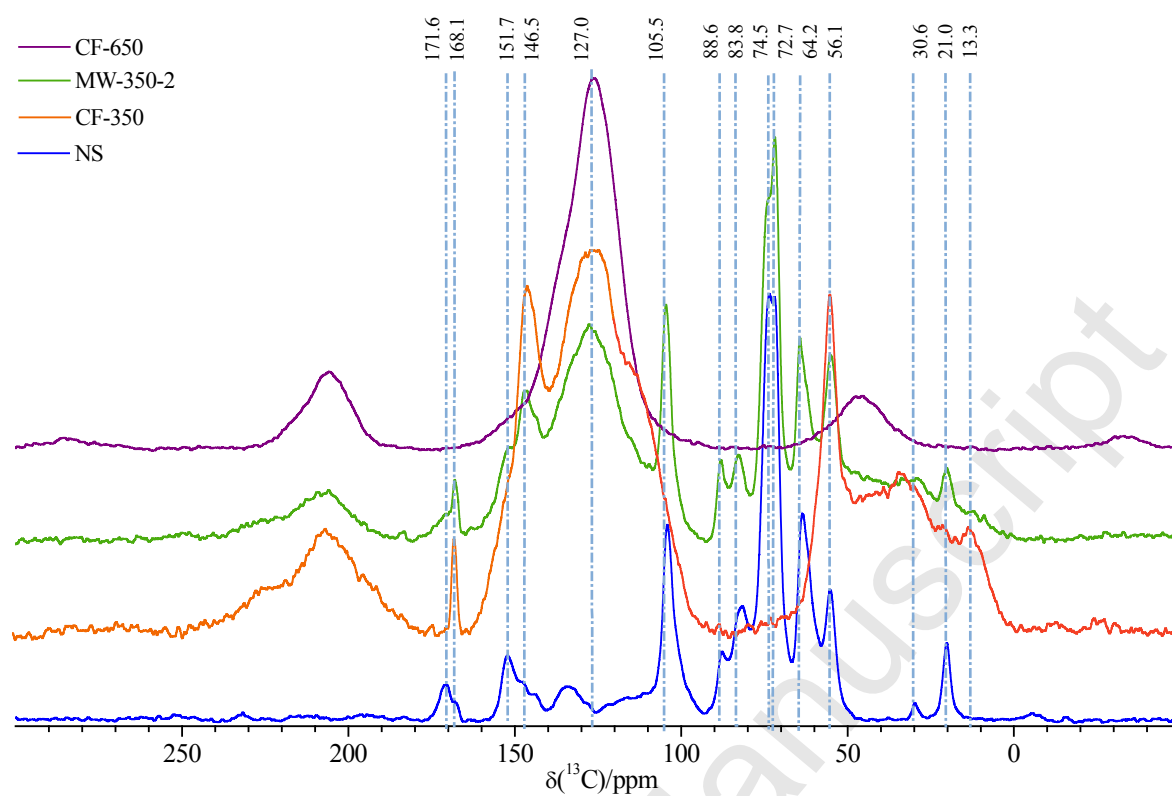


Fig. 3

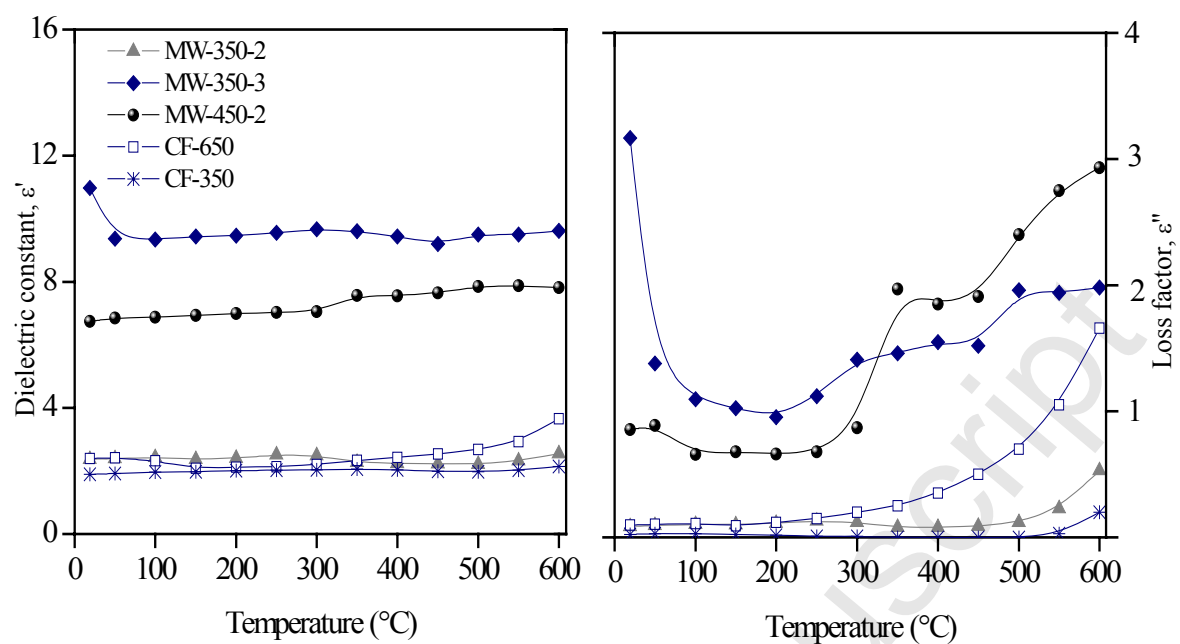


Fig. 4

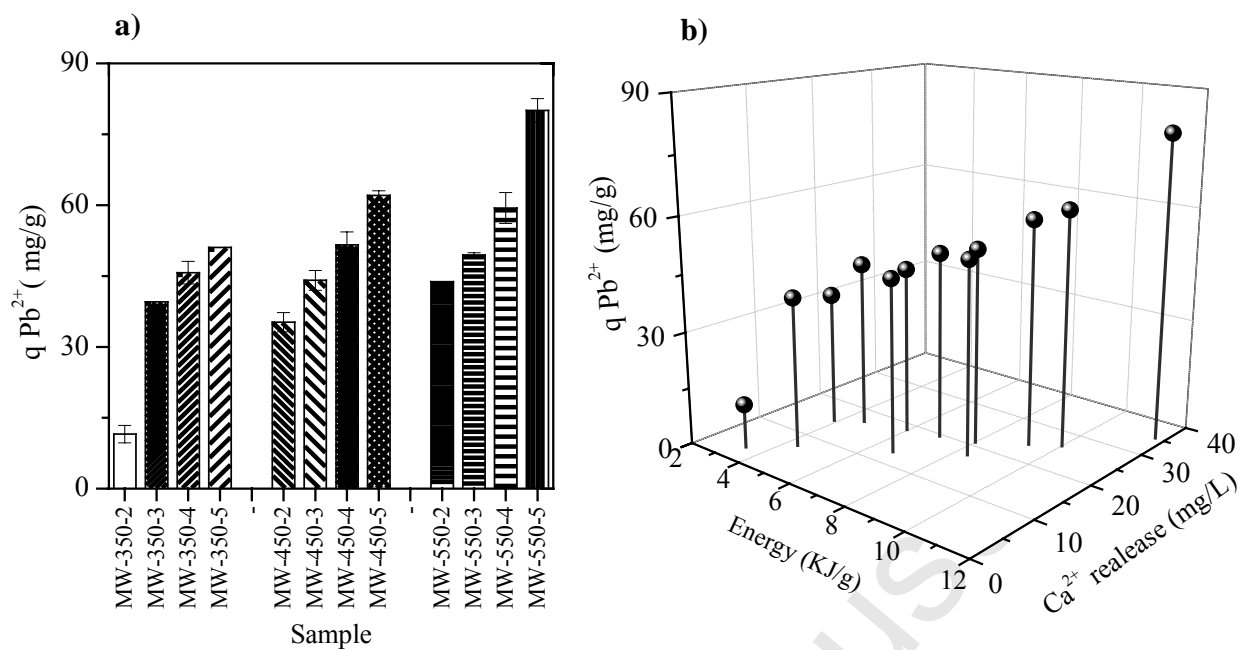
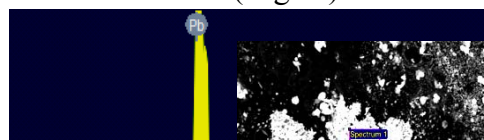
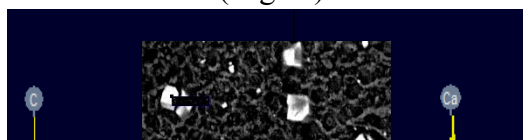
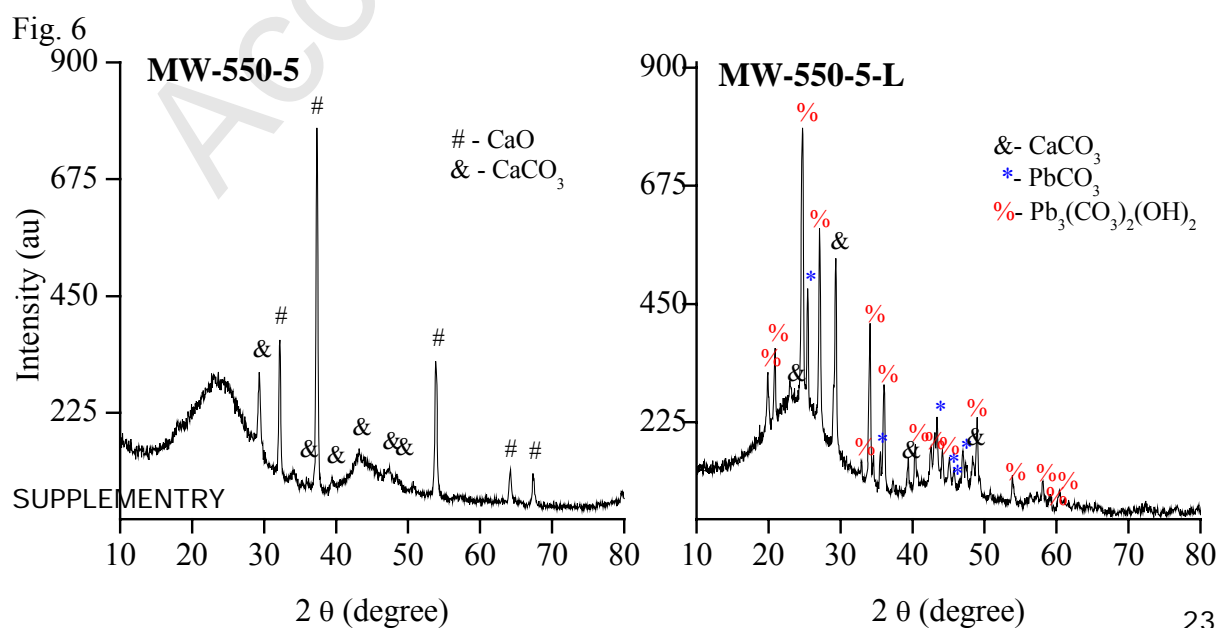
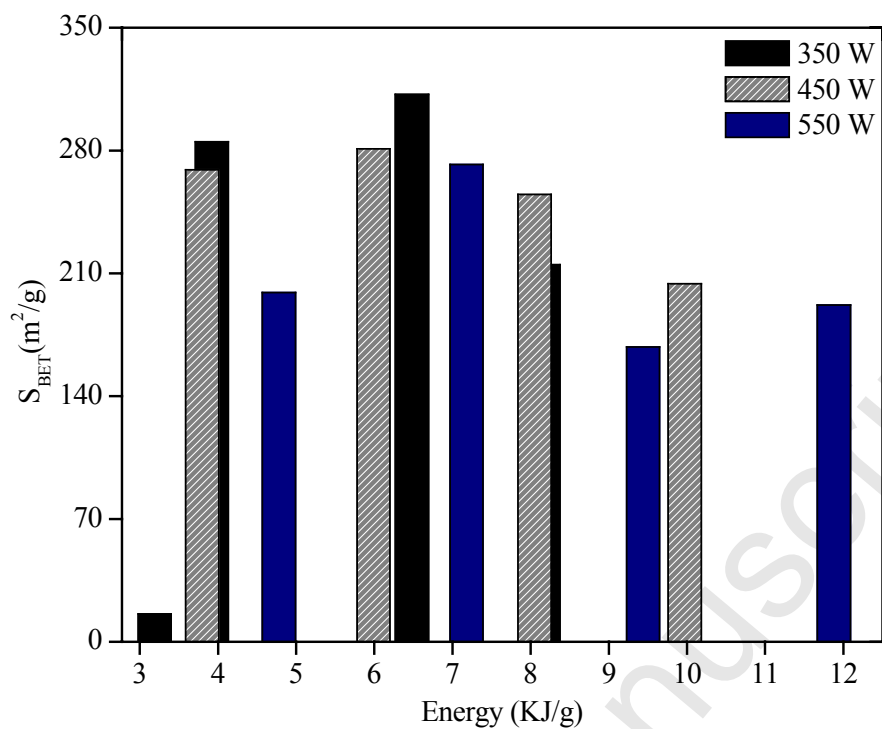


Fig. 5



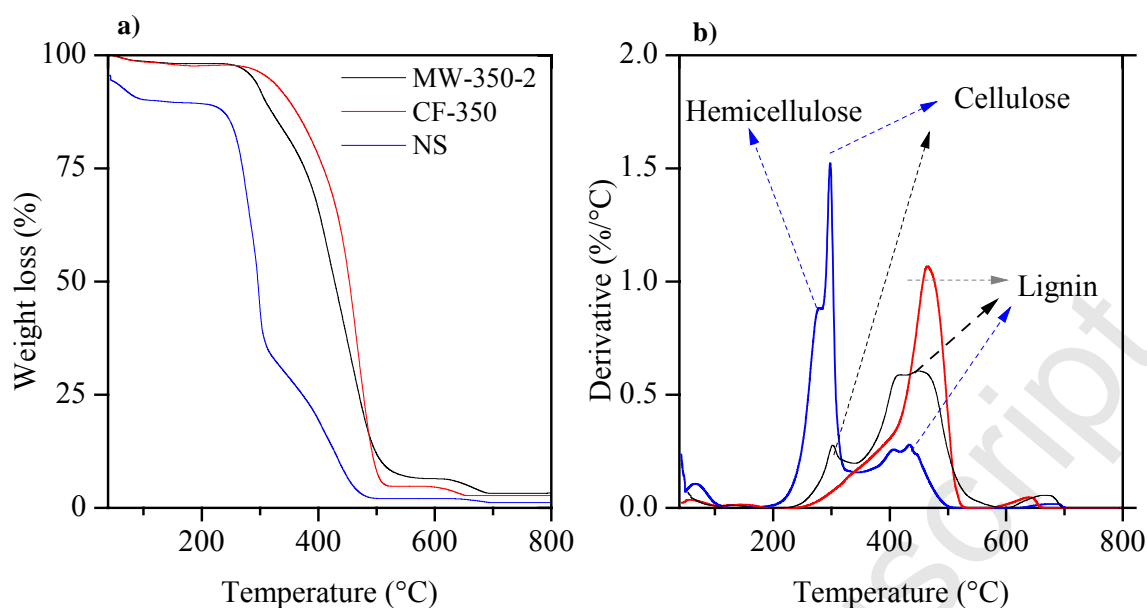


Fig. S1 TG and DTG curves in air atmosphere of pecan nutshell (NS), microwave carbon sample (MW-350-2) and conventional carbon sample (CF-350).

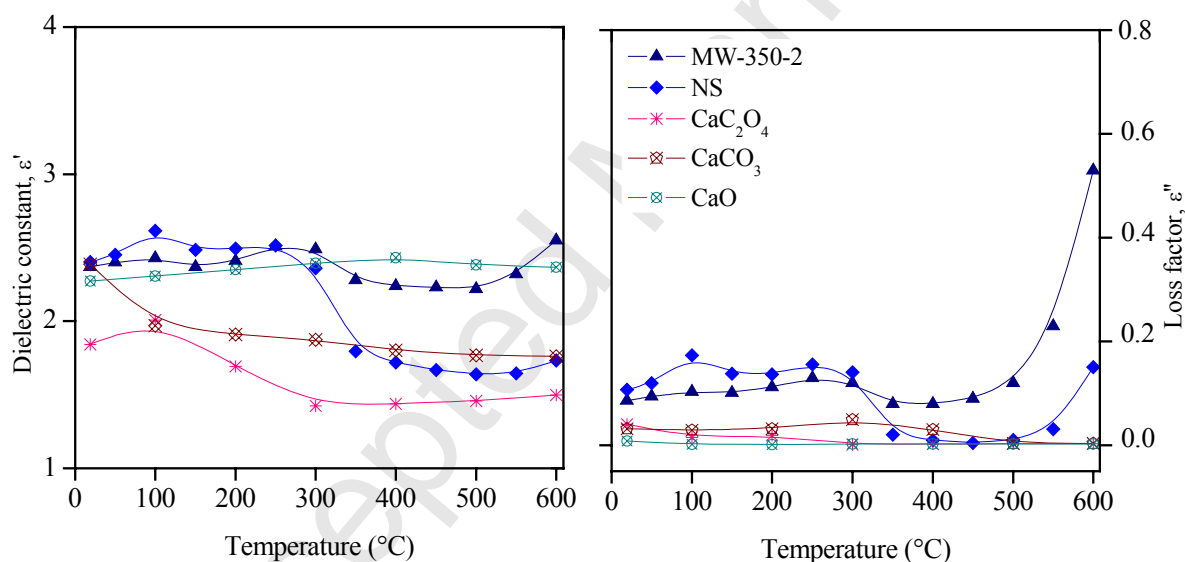


Fig. S2 Dielectric properties of inorganic compounds in carbonaceous samples.

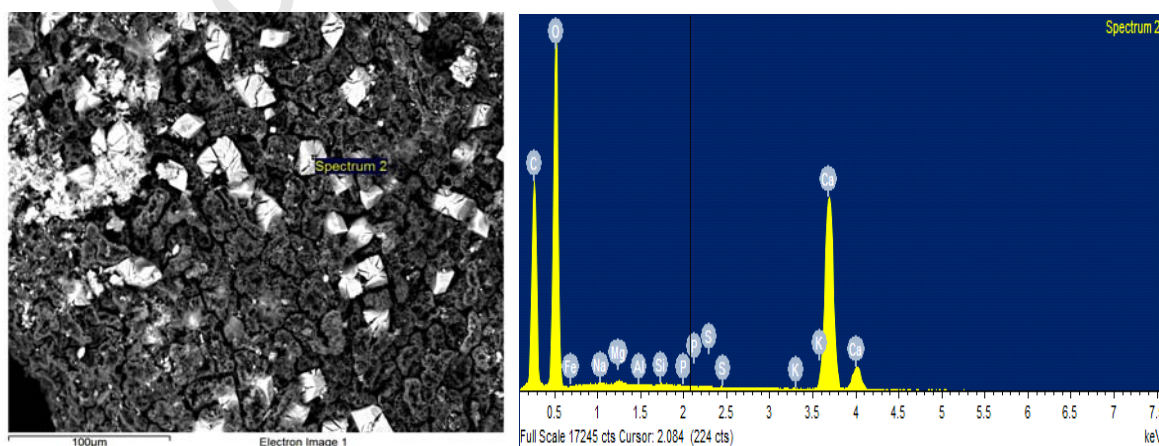


Fig. S3. SEM/EDX of the carbon-based samples MW-450-5

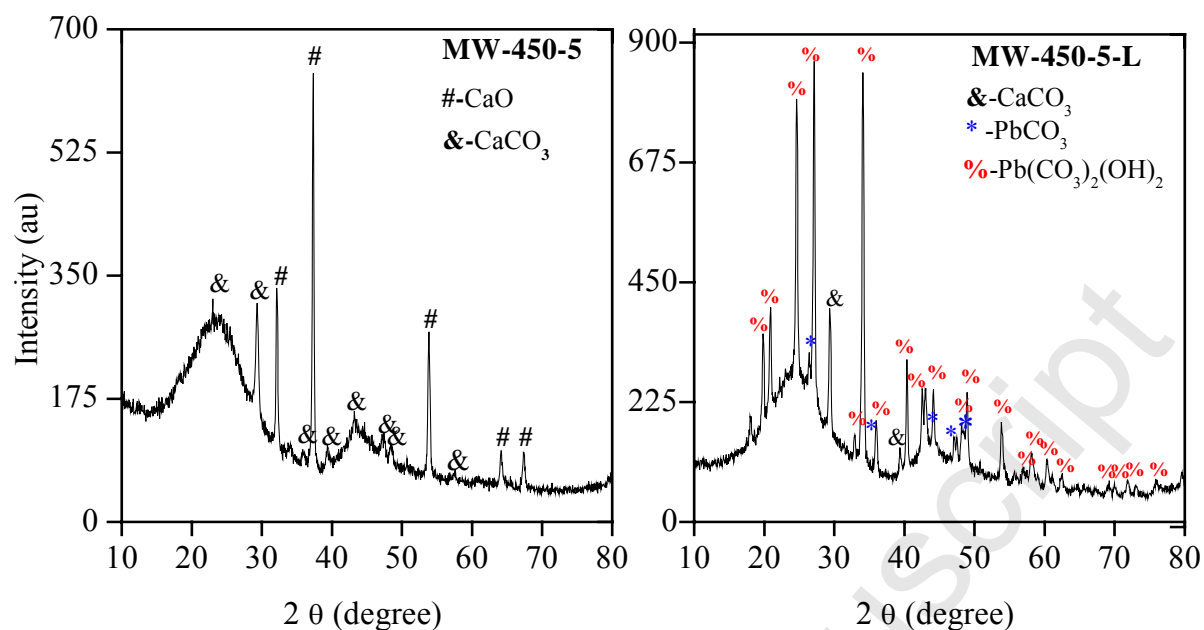


Fig. S4. XRD of the carbon-based samples MW-450-5 and of the same sample loaded with Pb²⁺ (MW-450-5-L)

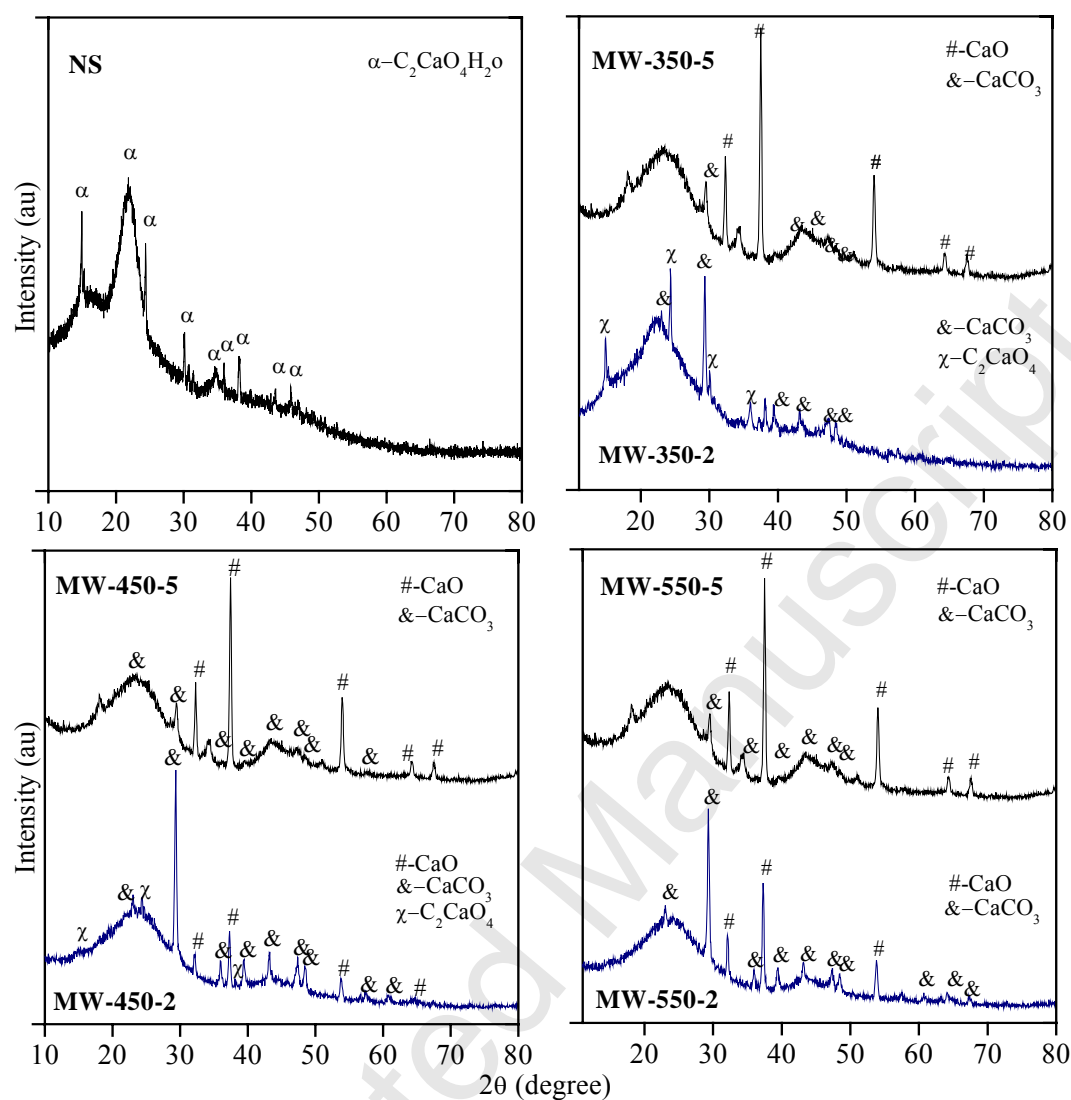


Fig. S5 XRD patterns of NS and carbon-based samples at 350, 450 and 550 W for 2 and 5 min respectively.

837
838

Table S1. Textural parameters of carbonaceous materials

Sample	$S_{\text{BET}}, \text{m}^2 \text{g}^{-1}$	$V_{\text{tot}}, \text{cm}^3 \text{g}^{-1}$	$V_{\text{mic}}, \text{cm}^3 \text{g}^{-1}$	$V_{\text{mes}}, \text{cm}^3 \text{g}^{-1}$	% Micro	% Meso
MW-350-2	16	0.0167	0.0016	0.0152	9.3	90.6
MW-350-3	285	0.1810	0.1373	0.0437	75.8	24.1
MW-350-4	312	0.1946	0.1527	0.0419	78.4	21.5
MW-350-5	215	0.1273	0.1027	0.0246	80.6	19.3
MW-450-2	269	0.1602	0.1286	0.0316	80.2	19.7
MW-450-3	281	0.1702	0.1390	0.0312	81.6	18.3
MW-450-4	255	0.1580	0.1211	0.0369	76.6	23.3
MW-450-5	204	0.1277	0.0967	0.0310	75.7	24.2
MW-550-2	199	0.1129	0.0993	0.0136	87.9	12.0
MW-550-3	272	0.1726	0.1310	0.0416	75.9	24.1
MW-550-4	168	0.1143	0.0875	0.0268	76.5	23.4
MW-550-5	192	0.1306	0.0933	0.0373	71.4	28.5

839
840
841
842
843